Proactive pipe management: Multiaxial fatigue of water pipe grey cast iron

Edward John[1], Joby Boxall[1], Richard Collins[1], Elisabeth Bowman[1], and Luca Susmel[1]

[1]Department of Civil and Structural Engineering, The University of Sheffield, Sheffield, UK

Author correspondence: edajohn1@sheffield.ac.uk

Abstract

The UK's water distribution networks contain large numbers of decades-old Grey Cast Iron (GCI) water pipes which are well known to deteriorate in service, develop leaks and ultimately burst. Reducing leakage has become a priority for UK water companies to provide a resilient water service in the face of climate change, population growth and other pressures. The huge number of GCI water pipes still in service coupled with very low pipe replacement rates mean the remaining GCI pipes cannot be replaced wholesale. This paper makes use of recently published multiaxial fatigue data for GCI pipes to investigate whether the multiaxial combination of loads experienced by a GCI water pipe could be used to identify pipes at a greater risk of failure. Based on a comparison of loading scenarios, this study concluded that considering the multiaxial combination of loads applied to a pipe does have the potential to help inform pipe replacement decisions, enabling high-risk pipes to be prioritised for replacement.

Keywords: Cast iron water pipes; multiaxial fatigue; fatigue testing; high-cycle fatigue; fatigue life estimation.

1. Introduction

Pipes made of Grey Cast Iron (GCI) are common in many UK water distribution networks, and around the world, and are often identified as having high failure rates compared to other pipe materials [1]. The UK water industry has committed to halving leakage rates by 2050, compared to 2018 levels [2], but only replaces around 0.1 % of pipes per year [3]. As a result, old GCI pipes will not be completely removed from service in the foreseeable future. To help reduce leakage rates in a cost-effective way techniques must be developed which enable targeted replacement of old GCI water pipes before they start leaking [2]. Figure 1 shows an example of GCI pipe that was exhumed after it had developed a leak.

GCI water pipes are vulnerable to corrosion which can result in the formation of localised pits or uniform wall loss [4]. The reduction in wall thickness caused by corrosion increases the stresses experienced by the pipe material and can lead to the formation of leaking cracks under service loading [5]. Smaller diameter GCI pipes can experience biaxial stress states; internal water pressure causes a pipe to experience stress acting around its circumference [6], whereas bending loads, such as vehicles and soil moisture response, cause stress acting in the pipe's axial direction [7, 8]. These loads are also time variable with the potential to cycle tens of times per day [9, 10] and frequently result in stress histories with a non-zero mean stress [10, 11].

In certain circumstances, the cause of GCI water pipe leakage may be high-cycle fatigue cracking due to multiaxial loading [11, 12]. Corrosion of GCI water pipes has been extensively researched [4, 13] but the fatigue response of the pipe material is less well understood and fundamental research is required to address this gap. Due to the focus of this work on replacing pipes before any leakage can occur, the fatigue processes of interest are crack initiation and growth to a size that allows water loss.

Uniaxial fatigue loading refers to a time variable stress or strain applied to a material in a single direction. Previous fatigue testing of water pipe GCI has been predominantly uniaxial [12, 14]. Cases where stresses or strains act in more than one direction are referred to as multiaxial fatigue loading. Different materials respond to multiaxial loading in different ways meaning this type of fatigue loading cannot usually be analysed using uniaxial fatigue models [15]. Multiaxial fatigue models are used to predict how a given material will respond to a particular multiaxial fatigue stress history, however, a wide range of these models are available and so it is important to validate a model for the material of interest, preferably using experimental data [16-18].

Comparing the relative fatigue damage caused by the multiaxial load history experienced by different GCI water pipes could be used to help select which pipes to replace, enabling water utility pipe replacement budgets to be spent more efficiently. However, this has not been possible because no multiaxial fatigue model had been calibrated and validated for water pipe GCI due to a lack of suitable fatigue data. Recently, the current authors addressed this gap by using an extensive series of fatigue test data to identify a suitable fatigue criterion for water pipe GCI, as detailed by John et al. [19] and summarised in the following section. The study detailed in this paper aimed to build on this recent work by investigating whether the multiaxial combination of loads experienced by GCI water pipes could be used to identify pipes at a greater risk of failure. This was achieved by using the multiaxial fatigue criterion validated by John et al. [19] to compare the damaging effect of two different buried pipe loading scenarios.

2. Multiaxial Fatigue of Water Pipe GCI

The work summarised in this section was first reported by John et al. [19] in International Journal of Fatigue. The aim of the work was to identify a fatigue criterion that was able to predict the multiaxial High-Cycle Fatigue (HCF) response of water pipe GCI. Due to the lack of multiaxial fatigue data available for GCI, a programme of fatigue experiments was carried out to provide the data needed to select a suitable criterion. In this section, the fatigue criteria that were tested are introduced. Then, the process used to generate the experimental data required to calibrate and validate the fatigue criteria are described. To validate each criterion the predictions made by the calibrated criteria were then compared with the experimental fatigue data.

2.1. Fatigue criteria

Due to the reported effectiveness of stress-based, critical plane, multiaxial fatigue criteria when predicting HCF cycles to failure [16], four different variants of this type of criteria were tested. The Smith-Watson-Topper (SWT) [20] and Modified Marquis-Socie (MMS) [21] criteria both assume that fatigue crack growth is dominated by tensile crack opening. Both these criteria only require a fully-reversed uniaxial fatigue curve for calibration. The Carpinteri–Spagnoli (CS) criterion [22] and Modified Wöhler Curve Method (MWCM) [23] consider both the normal and shear stresses acting on the critical plane allowing them to be calibrated for different cracking modes. The expense of this flexibility is that these two criteria require the fully-reversed uniaxial and torsional fatigue curves for calibration, and the MWCM also requires a mean-stress uniaxial fatigue curve. The mathematical expression for each of these fatigue criteria can be found in John et al. [19].

2.1. Fatigue testing

The experiments conducted by John et al. [19] aimed to generate the data required to calibrate the four fatigue criteria introduced above and test the ability of these criteria to predict the multiaxial fatigue behaviour of water pipe GCI. The stresses applied for this testing were intended to be straightforward to apply and provide a good test for the multiaxial fatigue criteria, rather than to closely replicate realistic water pipe loading. A combination of tensile and torsional loads was used.

GCI water pipes are no longer manufactured and exhumed water pipes are often heavily corroded [24]. It is also difficult to obtain large amounts of metallurgically similar pipe material and produce torsional specimens from pipe walls. To overcome these challenges, tubular fatigue specimens were produced from 16 new BS416-2 [25] soil pipes sourced from the same foundry (Hargreaves Foundry, Halifax, UK). These pipes have very similar graphitic microstructures, tensile stress-strain, and fatigue properties to water pipes [19, 26].

The uniaxial $R = -1$, uniaxial $R = 0.1$, and torsional $R = -1$ fatigue curves (where R = min. stress / max. stress) were required for calibration purposes. To characterise these curves with sufficient certainty, five stress levels were tested with two repeats per stress level. Data from combined tension and torsion (TT) loading was used to test the fatigue criteria because this type of loading generates complex multiaxial stress histories. To provide both proportional and non-proportional multiaxial stresses specimens were testing using tension-torsion in-phase (TTIP) loading and tension-torsion 90° out-of-phase (TTOOP) loading. For these multiaxial loadings the aim was to generate some data points across a range of stress amplitudes to compare against the model predictions, not to characterise the curves fully, so three stress levels were tested with five specimens.

Examples of failed specimens under different loading conditions are shown by Figure 2. Key observations were that the material demonstrated sensitivity to mean stresses and that for TT loading the addition of a tensile load had a damaging effect relative to pure torsion. The different phasing of the TT loads appears to have had no clear effect.

2.2. Fatigue criteria validation

The SWT, MMS, CS, and MWCM fatigue criteria were used to predict the cycles to failure of each fatigue test. The fatigue criteria predicted cycles to failure are plotted against the measured cycles to failure in Figure 3 for all load types. The effectiveness of each fatigue criterion was quantified using the mean square error quantity, T_{RMS}, as detailed by Walat and Łagoda [27].

The two TT load types (TTIP and TTOOP) were the only data not used to calibrate any fatigue criteria, while the uniaxial $R = 0.1$ data was only used to calibrate the MWCM. To compare the effectiveness of the fatigue criteria T_{RMS} values were calculated for the TT loadings for each fatigue criterion ($T_{RMS,TT}$) and also for uniaxial $R = 0.1$ loading ($T_{RMS,M}$), but for only the SWT, MMS and CS criteria. These T_{RMS} values are given in Figure 3.

The predicted cycles to failure for each multiaxial fatigue criterion are plotted against the experimentally observed cycles to failure for each specimen in Figure 3. Data points which fall on the solid diagonal line indicate perfect prediction. The dash-dot lines show the 10% and 90% probability of survival scatter bands derived from the uniaxial R = -1 experimental data. If all predictions for a given loading condition fall within these scatter bands then the prediction error is effectively no worse than the experimentally observed scatter. The T_{RMS} values shown on Figure 3 for each criterion quantify the effectiveness of each criterion. For example, for both the SWT and CS criteria all the uniaxial R = 0.1 predictions fall within the scatter bands, however, the SWT criteria predictions are closer to the perfect prediction line. In reflection of this, the $T_{RMS,M}$ value for the SWT is lower than the CS value (3.3 compared to 11.5) indicating the SWT provides better predictions for this data set.

All four fatigue criteria investigated were able to provide reasonable fatigue life predictions for the GCI pipe material investigated with a very small number of data points falling outside the scatter bands for each criterion, as shown by Figure 3. The MMS criterion offered the best multiaxial fatigue predictions ($T_{RMS,TT}$ = 5.6), closely followed by the CS and SWT criteria ($T_{RMS,TT}$ = 6.2 and $T_{RMS,TT}$ = 6.7 respectively). However, both the MMS and CS criteria were unable to accurately predict the mean stress effect ($T_{RMS,M}$ = 22.8 and $T_{RMS,M}$ = 11.5 respectively) while the SWT criterion was able to predict this well ($T_{RMS,M}$ = 3.3) without needing mean stress calibration data. A significant proportion of the stress cycles experienced by GCI water pipes are thought to feature non-zero mean stresses [10, 11], therefore, the SWT criterion was considered to provide the best overall fatigue life predictions for multiaxial fatigue of water pipe GCI in the HCF regime.

3. Methods

A multiaxial loading comparison was performed to test the sensitivity of the SWT criterion to multiaxial stresses reflective of in-service loading experienced by small-diameter GCI water pipes. To test this sensitivity two load conditions were considered: uniaxial loading and out-of-phase equibiaxial loading (see Figure 4). Uniaxial fatigue loading could reflect a pipe experiencing internal water pressure fluctuations, while equibiaxial fatigue loading could result from the same water pressure loading with the addition of bending caused by heavy road vehicles.

Reflecting the fact that fatigue stresses experienced by water pipes frequently feature a non-zero mean, the uniaxial stress was characterised by a stress amplitude of 65 MPa with a load ratio of R = 0.1 (see Figure 4b). The stress amplitude was chosen so that the predictions made using the SWT criterion were within the range the criterion had been validated for. To isolate the effect of an added biaxial stress, the biaxial condition featured a fatigue stress identical to the uniaxial stress in one direction (σ_a = 65 MPa, R = 0.1), but an additional fatigue stress was also applied perpendicular to this (see Figure 4c). So that both stresses would be equally damaging independently, the additional perpendicular fatigue stress was characterised by the same amplitude and load ratio (σ_a = 65 MPa, R = 0.1). To reflect a very simplistic alternating biaxial loading the two stresses were assumed to occur exactly out-of-phase. In other words, when the stress in one direction was at its maximum value the stress in the other direction was at its minimum, and vice versa. To test the sensitivity of the SWT fatigue criterion to the added biaxial stress predictions were made using this criterion for both load cases.

Using the same approach as John et al. [19], the SWT criterion was applied in a linear-elastic form [28]:

$$\sigma_{a,R=-1} = \sqrt{\sigma_{n,max} E \varepsilon_{n,a}} \quad \textbf{(1)}$$

where: $\sigma_{a,R=-1}$ is the equivalent uniaxial fully reversed stress amplitude; $\sigma_{n,max}$ is the maximum value of normal stress on the critical plane; E is the material's elastic modulus; and $\varepsilon_{n,a}$ is the normal strain amplitude on the critical plane. The critical plane is that experiencing the maximum value of $\varepsilon_{n,a}$. To apply the SWT criterion using a stress-based approach the normal strain on an aribtrary material plane, $\varepsilon_{X'}$, multiplied by the material elastic modulus, may be calculated from the plane's stresses at any point during a load history using Hooke's law:

$$E\varepsilon_{X'}(t) = \sigma_{X'}(t) - \nu[\sigma_{Y'}(t) - \sigma_{Z'}(t)] \quad \textbf{(2)}$$

where: $\sigma_{X'}$, $\sigma_{Y'}$ and $\sigma_{Z'}$ are the stresses acting on an arbitrary material plane defined by the axes X', Y', Z' where X' is normal to the plane; ν is the material's Poisson ratio; and t is time. $E\varepsilon_{n,a}$ is calculated from $E\varepsilon_{X'}(t)$ for each plane, and the critical plane is that which features the maximum value of $E\varepsilon_{n,a}$. Cycles to failure are predicted using equation (3):

$$N_f = N_A \left(\frac{\sigma_{A,R=-1}}{\sigma_{a,R=-1}}\right)^k \quad \textbf{(3)}$$

where: N_A is the high-cycle reference cycles to failure; $\sigma_{A,R=-1}$ is the uniaxial fully reversed reference stress amplitude, determined at N_A cycles to failure; and k is the uniaxial fully reversed negative inverse slope. The values used for $\sigma_{A,R=-1}$ and k were 85.8 MPa and 11.5, respectively [19].

4. Results

The SWT criterion predicted cycles to failure for the uniaxial and out-of-phase equibiaxial fatigue scenarios are plotted in Figure 5. The cross on this figure indicates the number of cycles corresponding to a predicted probability of survival (P_S) of 50%, while the bars show the range between the P_S = 90% and P_S = 10% cycles, assuming the same degree of scattering observed for the uniaxial R=-1 experimental data. The overlap of the scatter bars indicates that a pipe experiencing out-of-phase equibiaxial loading is not guaranteed to fail sooner than if it were experiencing uniaxial loading. However, the average cycles to failure and scatter range for out-of-phase equibiaxial loading is shifted downward by 74% relative to uniaxial loading, meaning that pipes experiencing out-of-phase equibiaxial loading are predicted to have a higher probability of failing first. Considering the predicted average values, 50% of the time uniaxial loading failures are predicted to occur by 2.47×10^5 load cycles, whereas this value drops to 6.54×10^4 load cycles for out-of-phase equibiaxial loading.

5. Discussion

The predicted 74% reduction in average fatigue life for equibiaxial loading does not mean that a real pipe's total years-to-failure would be reduced by an average of 74%; fatigue damage accumulation can only begin once corrosion pits have grown to a sufficiently damaging size [11, 12]. However, the predicted reduction of average load cycles to failure of 74% does indicate that water pipe GCI is likely to be sensitive to biaxial fatigue loading and that biaxial fatigue loads have the potential to cause more damage, and therefore result in earlier failures, than either load independently. The practical implication of this is that, for a small-diameter pipeline with internal water pressure fluctuations, an individual pipe buried under a road used regularly by heavy vehicles has a greater chance of developing a fatigue crack before another pipe in the same pipeline that is away from the road, if all other conditions are identical. Uniaxial fatigue assessment alone could not have been used to make this distinction.

Many GCI water pipes suffer from irregular corrosion pitting which may significantly affect the fatigue response of biaxially loaded pipes by behaving as stress concentrating notches. Therefore, before water utility asset managers are able to use pipe loading conditions to inform pipe replacement decisions a deeper understanding is needed of the interaction between biaxial fatigue loads and the irregular corrosion pitting commonly found in GCI pipes. To address this gap, a unique experiment has been developed at the University of Sheffield that is able to simultaneously apply bending and internal water pressure fatigue loads to small diameter pipes (see Figure 6a). This experiment is being used to investigate how different corrosion pit shapes and biaxial fatigue load combinations affect the fatigue life and failure mode of GCI pipes. This experiment is also providing an insight into the very early stages of leak development, which usually occur unseen underground. An example of a fatigue-induced leak in a pitted pipe generated using this experiment is shown in Figure 6b.

6. Summary

The work detailed in this paper aimed to investigate whether the multiaxial fatigue loading experienced by Grey Cast Iron (GCI) water pipes could be used to inform pipe replacement decisions. The findings of this paper show that considering the multiaxial combination of loads applied to a pipe has the potential to help inform pipe replacement decisions where the aim is to prevent leakage. Applying the validated SWT multiaxial fatigue criterion to a simplistic but realistic scenario has shown that a small-diameter pipe buried under a road and subject to water pressure loading has a greater chance of developing a fatigue crack before a neighbouring pipe away from the road if all other conditions are identical. Uniaxial fatigue assessment alone could not have been used to make this distinction. Further investigation is required to fully understand the effect of fatigue load combinations and how these interact with other factors such as corrosion pitting.

Acknowledgements

This work was funded by UK Water Industry Research (UKWIR) and the ESPRC through the Water Infrastructure and Resilience (WIRe) Centre for Doctoral Training (EP/S023666/1). The authors would like to thank the technicians Paul Blackbourne, Mario Dorna, Chris Todd, and Richard Kay for their work which enabled the fatigue testing to take place.

References

[1] N.A. Barton, T.S. Farewell, S.H. Hallett, T.F. Acland, "Improving pipe failure predictions: Factors affecting pipe failure in drinking water networks". Water Resources, Vol. 164, 2019.

[2] J. Sanders, D. Marshallsay, G. Mountfort, G. Fox, M. Butler, "A Leakage Routemap to 2050". Water UK, 2022. https://www.water.org.uk/news-item/milestone-leakage-routemap-to-revolutionise-the-reduction-of-leakage-from-pipes/ (accessed June 15, 2022).

[3] Economic Insight Ltd, "Options for a sustainable approach to asset maintenance and replacement". 2022. https://www.water.org.uk/news-views-publications/publications/options-sustainable-approach-asset-maintenance-and-replacement (accessed September 11, 2023).

[4] Z. Soltani Asadi, R.E. Melchers, “Long-term external pitting and corrosion of buried cast iron water pipes”. Corrosion Engineering Science and Technology, Vol. 53, 2018.

[5] J. Farrow, D. Jesson, M. Mulheron, T. Nensi, P. Smith, “Achieving zero leakage by 2050: The basic mechanisms of bursts and leakage”. UK Water Industry Research, 2017.

[6] M. Larson, L. Jönsson, “Elastic Properties of Pipe Materials during Hydraulic Transients”. Journal of Hydraulic Engineering, Vol. 117, 1991.

[7] D. Chan, C.P.K. Gallage, P. Rajeev, J. Kodikara, “Field performance of in-service cast iron water reticulation pipe buried in reactive clay”. Canadian Geotechnical Journal, Vol. 52, 2015.

[8] C. Randeniya, D.J. Robert, C.Q. Li, J. Kodikara, “Large-scale experimental evaluation of soil saturation effect on behaviour of buried pipes under operational loads”. Canadian Geotechnical Journal, Vol. 57, 2020.

[9] Department for Transport, “AADF Data - major and minor roads”, Gov.Uk, 2020. https://roadtraffic.dft.gov.uk/downloads (accessed April 19, 2021).

[10] C. Jara-Arriagada, I. Stoianov, “High resolution water pressure monitoring for the assessment of fatigue damage in water pipes”. 2nd International Joint Conference on Water Distribution Systems Analysis and Control in the Water Industry, Valencia, 2022.

[11] W. Brevis, L. Susmel, J. Boxall, “Investigating in-service failures of water pipes from a multiaxial notch fatigue point of view: A conceptual study”. Proceedings of the Institution of Mechanical Engineers, Part C: Journal of Mechanical Engineering Science, Vol. 229, 2015.

[12] R. Jiang, S. Rathnayaka, B. Shannon, X.-L. Zhao, J. Ji, J. Kodikara, “Analysis of failure initiation in corroded cast iron pipes under cyclic loading due to formation of through-wall cracks”. Engineering Failure Analysis, Vol. 103, 2019.

[13] R.E. Melchers, R.B. Petersen, T. Wells, “Empirical models for long-term localised corrosion of cast iron pipes buried in soils”. Corrosion Engineering Science and Technology, Vol. 54, 2019.

[14] J.B. Kommers, “The static and fatigue properties of some cast irons”. Proceedings of the American Society for Testing Materials, Vol. 28, 1928.

[15] D.F. Socie, G.B. Marquis, “Multiaxial Fatigue”. Society of Automotive Engineers, Inc., Warrendale, Pa., 1999.

[16] A. Fatemi, N. Shamsaei, “Multiaxial fatigue: An overview and some approximation models for life estimation”. International Journal of Fatigue, Vol. 33, 2011.

[17] D.F. Socie, “Multiaxial fatigue damage models”. Journal of Engineering Materials and Technology, Transactions of the ASME, Vol. 109, 1987.

[18] E. Santecchia, A.M.S. Hamouda, F. Musharavati, E. Zalnezhad, M. Cabibbo, M. El Mehtedi, S. Spigarelli, “A Review on Fatigue Life Prediction Methods for Metals”. Advances in Materials Science and Engineering, Vol. 2016, 2016.

[19] E. John, J. Boxall, R. Collins, E. Bowman, L. Susmel, “Multiaxial fatigue of water pipe grey cast iron”. International Journal of Fatigue, Vol. 178, 2024.

[20] P. Smith, K.N., Topper, T.H., Watson, “A stress–strain function for the fatigue of metals”. Journal of Materials, Vol. 5, 1970.

[21] G.B. Marquis, P. Karjalainen-Roikonen, “Long-life multiaxial fatigue of a nodular graphite cast iron”. Biaxial/Multiaxial Fatigue and Fracture, 2003.

[22] A. Carpinteri, A. Spagnoli, S. Vantadori, “Multiaxial fatigue assessment using a simplified critical plane-based criterion”. International Journal of Fatigue, Vol. 33, 2011.

[23] L. Susmel, “Multiaxial notch fatigue: From nominal to local stress/strain quantities”. Woodhead Publishing Limited, Cambridge, 2009.

[24] H. Mohebbi, D.A. Jesson, M.J. Mulheron, P.A. Smith, “The fracture and fatigue properties of cast irons used for trunk mains in the water industry”. Materials Science and Engineering A, Vol. 527, 2010.

[25] British Standards Institution, “Discharge and ventilating pipes and fittings, sand-cast or spun in cast iron - Part 2: Specifications for socketless systems. BS 416-2:1990”. 1990.

[26] E. John, J. Boxall, R. Collins, E. Bowman, L. Susmel, “Investigating an alternative to exhumed grey cast iron water pipes for small-scale fatigue tests”. 2nd International Joint Conference on Water Distribution Systems Analysis & Computing and Control in the Water Industry, Valencia, Spain, 2022.

[27] K. Walat, T. Łagoda, “Lifetime of semi-ductile materials through the critical plane approach”. International Journal of Fatigue, Vol. 67, 2014.

[28] N.E. Dowling, C.A. Calhoun, A. Arcari, “Mean stress effects in stress-life fatigue and the Walker equation”. Fatigue and Fracture of Engineering Materials and Structures, Vol. 32, 2008.

Figure 1: Example of a leaking cast iron pipe from Barton et al. [1].

a) b) c)

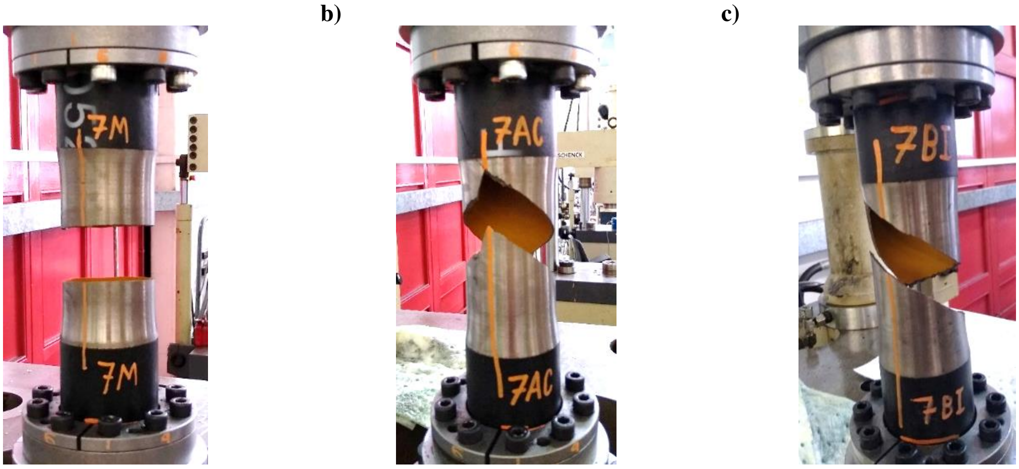

Figure 2: Examples of failed specimens tested under a) uniaxial loading, b) torsional loading, and c) out-of-phase tension-torsion loading from John et al. [19].

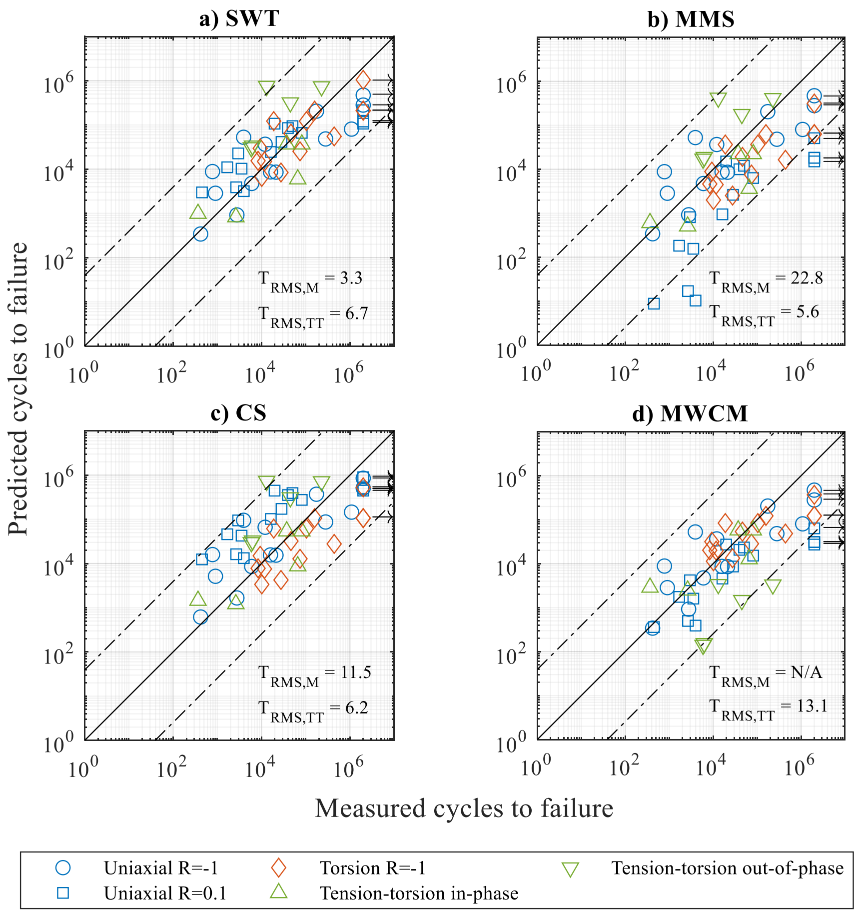

Figure 3: Predicted cycles to failure vs measured cycles to failure for four fatigue criteria from John et al. [19]. Dashed lines show the fully reversed uniaxial scatter band.

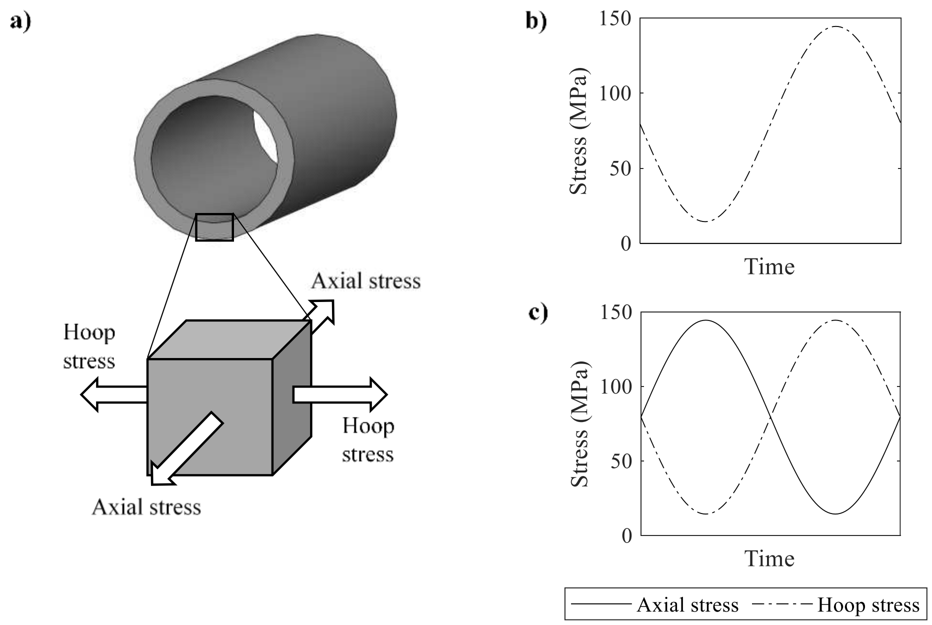

Figure 4: (a) Schematic showing hoop and axial stress directions relative to a pipe and plots of a single stress cycle for the (b) uniaxial and (c) out-of-phase equibiaxial scenarios.

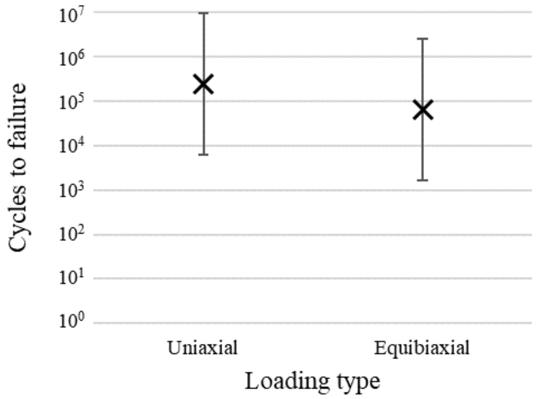

Figure 5: SWT criterion predicted cycles to failure for uniaxial loading and equibiaxial loading. The error bars show the range between the P_S=90% and P_S=10% cycles.

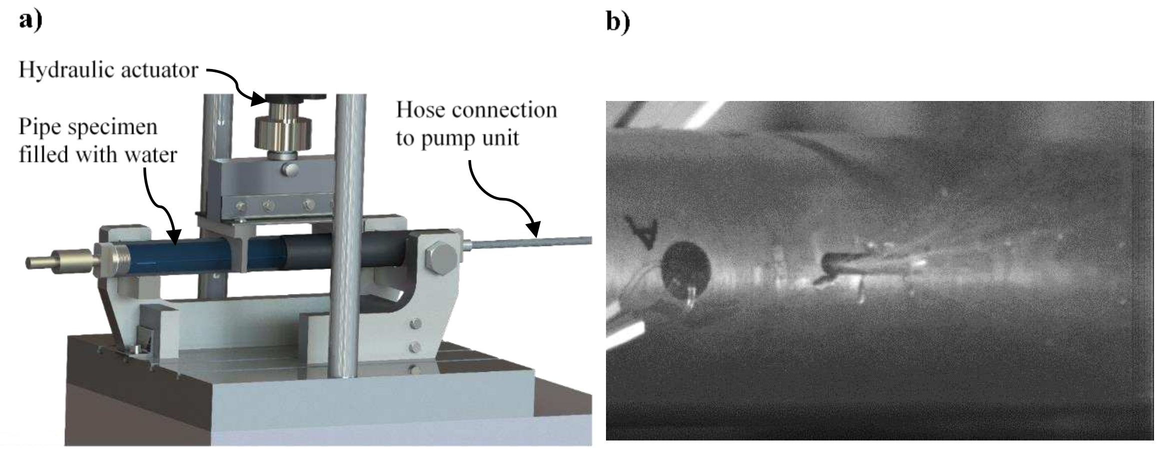

Figure 6: (a) Cutaway render of the pipe biaxial fatigue test apparatus which is able to apply four-point bending and internal water pressure fatigue loads, and (b) an image showing a pitted pipe leaking as a result of water pressure fatigue loading.